

# Structural transformations of silver photodoped Ge-Sb-Te thin films

S. KUMAR, D. SINGH, R. THANGARAJ\*

*Semiconductors Laboratory, Department of Physics, Guru Nanak Dev University, Amritsar-143005, India*

Photodoping of Ag in  $\text{Ge}_{22}\text{Sb}_{22}\text{Te}_{56}$  films has been done by illuminating the thermally evaporated Ag:Ge-Sb-Te bilayer (~40 nm:250 nm) with 500 W halogen lamp. Disappearance of Ag (111) peak in x-ray scan from the bilayer after 20 min. illumination at room temperature confirms the photodoping of Ag in the chalcogenide film. The effects of Ag-photodoping on the optical properties of the  $\text{Ge}_{22}\text{Sb}_{22}\text{Te}_{56}$  film have been examined by transmission and reflection data. The structural phases have been evaluated by x-ray diffraction patterns of thermally annealed films and sheet resistance variation with temperature measurements. It is found that amorphous to crystalline transformation temperature increases and optical gap decreases in Ag-photodoped films. The x-ray diffraction (XRD) has been studied for the films annealed at two different temperatures. Peaks of FCC phases appear in  $\text{Ge}_{22}\text{Sb}_{22}\text{Te}_{56}$  film annealed at 160 °C but Ag-photodoped  $\text{Ge}_{22}\text{Sb}_{22}\text{Te}_{56}$  film remains amorphous. The peaks of  $\text{Ag}_5\text{Te}_3$  phases are identified for Ag-photodoped  $\text{Ge}_{22}\text{Sb}_{22}\text{Te}_{56}$  film annealed at 250 °C.

(Received August 17, 2011; accepted September 15, 2011)

*Keywords:* Ge-SbTe, Thin films, Silver photodoping

## 1. Introduction

The chalcogenide alloy,  $\text{Ge}_2\text{Sb}_2\text{Te}_5$  (GST) has been commercially utilized as optical recording media for digital-versatile-disk (DVD)-RAM [1]. Currently, it is widely adopted as the active layer of phase-change random access memory (PRAM) due to its outstanding electronic performance. One peculiarity of  $\text{Ge}_2\text{Sb}_2\text{Te}_5$  and other materials on the pseudobinary GeTe-Sb<sub>2</sub>Te<sub>3</sub> line such as  $\text{Ge}_1\text{Sb}_2\text{Te}_4$  or  $\text{Ge}_1\text{Sb}_4\text{Te}_7$  is that they crystallize upon heating, first into a metastable rocksalt structure and then at higher temperatures into a stable hexagonal phase [2]. Doping is one of the most effective methods to improve the properties of phase change materials. Elements such as Bi, Zn, Ag, etc. have been doped into Ge-Sb-Te films to improve their characteristics [3-5]. These additives influence the network structure or short range ordering, but due to the phase segregation and clustering leads to the difficulty in fabricating thin films from multicomponent chalcogenide systems. Photodiffusion is one such process, where one can fabricate metal rich chalcogenide films with homogenous impurity profile without clustering of the constituting phases [6]. The incorporation of appreciable amounts of a metal in the chalcogenide material alters the composition and hence the structure and the physicochemical properties of the material. The photodiffusion process, kinetics, diffusion mechanism, diffusion profiles have been well characterized and exploited in optoelectronics (diffraction gratings, photonic Band gap structures and nanolithography) [7]. In the previous work we have investigated the effect of Ag on thermal properties of chalcogenide glasses [8-10], but in recent work, we have experimentally investigated the photodoping of Ag impurity in amorphous  $\text{Ge}_{22}\text{Sb}_{22}\text{Te}_{56}$  film and the effect of Ag-photodoping on the

microstructure, optical gap, crystalline temperature and FCC to HCP phase transformation of  $\text{Ge}_{22}\text{Sb}_{22}\text{Te}_{56}$  films.

## 2. Experimental

The alloy of  $\text{Ge}_{22}\text{Sb}_{22}\text{Te}_{56}$  was synthesized using 99.999% elemental Ge, Sb and Te sealed in quartz ampoule (length ~10 cm, internal diameter ~6mm) evacuated to  $\sim 10^{-5}$  mbar. The melt was homogenized at 1373 K, at a rate of 4-5 °C/min for at least 48 h and finally cooled the sample. Cooling was done by switching off the furnace leaving the ampoule inside. Ampoule was taken out of the furnace at room temperature and broken carefully to extract the sample. Peaks of GST were identified in the x-ray scan of above prepared alloy. Using this source alloy, thin films of approximately 250 nm thick were prepared by thermal evaporation method using Hind High Vacuum Coating Unit (Model No. 12A4D). Well cleaned glass slides were used as substrates. The substrates were maintained at room temperature during the deposition and the pressure in the chamber during the deposition was below  $10^{-5}$  mbar. The films were left inside the chamber for ~24 h to attain metastable equilibrium as suggested by Abkowitz [11].

Then, ~40 nm silver film was evaporated on the top of the previously grown amorphous films to form Ag:Ge-Sb-Te bilayer geometry and Ag was photodiffused in these films by illuminating samples normally with halogen lamp (500 W) from silver side in Ag:Ge-Sb-Te bilayer for 20 min. at room temperature. Disappearance of Ag (111) peak in x-ray scan from bilayer geometry confirms the photodiffusion of Ag metal in chalcogenide film. After the diffusion processes were complete, the remnant Ag on the film surface was dissolved in 0.1N solution of  $\text{Fe}(\text{NO}_3)_3$

[12]. The crystal structure of bulk alloy, the amorphous nature of as-deposited  $\text{Ge}_{22}\text{Sb}_{22}\text{Te}_{56}$ , Ag-photodoped  $\text{Ge}_{22}\text{Sb}_{22}\text{Te}_{56}$  films and the annealed films at two different temperatures were identified by using  $\text{Cu-K}\alpha$  lines of x-ray-diffraction studies. A change in sheet resistance as a function of annealing temperature and amorphous-crystalline transformation temperatures of the samples were measured with a two-point probe. The sheet resistance measurements were done in vacuum chamber having pressure  $\sim 10^{-4}$  mbar and the values were averaged after three time measurements. The temperature at which an abrupt drop in the resistance takes place was taken as amorphous-crystalline transformation temperature. The transmittance ( $T$ ) w.r.t. air and specular reflectance ( $R$ ) of thin films were measured at room temperature using UV-VIS-NIR spectrophotometer (Perkin Elmer 950) in the wavelength range 400–3000 nm.

### 3. Results and discussion

X-ray diffraction studies are used for the confirmation of photodiffusion of Ag in amorphous chalcogenide film of  $\text{Ge}_{22}\text{Sb}_{22}\text{Te}_{56}$  [13]. Absence of any sharp peak in x-ray scans of the as deposited thermally evaporated  $\text{Ge}_{22}\text{Sb}_{22}\text{Te}_{56}$  films confirms the amorphous nature of the films as shown in curve b of Fig. 1. Two peaks of Ag having (111) and (200) planes [13] appears in x-ray scan of  $\sim 40\text{nm}$  Ag film deposited on the glass substrate (used as reference slide) as shown in Fig. 1 (c). Disappearance of Ag (111) in x-ray scan (curve e) from bilayer geometry (Ag:Ge-Sb-Te) after 20 min. illumination with halogen lamp confirms the photodiffusion of Ag in the amorphous chalcogenide film, as small peak of Ag (111) plane remains in the x-ray scan of as deposited bilayer of Ag:Ge-Sb-Te without illumination (curve d). Crystalline HCP phases of  $\text{Ge}_{22}\text{Sb}_{22}\text{Te}_{56}$  bulk alloy are also identified in the x-ray diffraction studies (curve a). The analysis of the x-ray diffraction data provides deeper understanding of amorphous to crystalline transformation exhibited in the sheet resistance measurements as discussed in the next section. Fig. 2 shows the diffractograms of annealed  $\text{Ge}_{22}\text{Sb}_{22}\text{Te}_{56}$  and Ag-photodoped  $\text{Ge}_{22}\text{Sb}_{22}\text{Te}_{56}$  at two different ( $160^\circ\text{C}$  and  $250^\circ\text{C}$ ) temperatures. Sharp peaks (200) and (220) (curve a) of  $\text{Ge}_{22}\text{Sb}_{22}\text{Te}_{56}$  film annealed at  $160^\circ\text{C}$  are identified as FCC structure of GST [5]. But the Ag-photodoped  $\text{Ge}_{22}\text{Sb}_{22}\text{Te}_{56}$  film annealed at  $160^\circ\text{C}$  (curve b) remains amorphous. So doping of Ag increases the crystalline temperature as Ag is a high melting temperature metal and will thus increase the crystalline temperature of  $\text{Ge}_{22}\text{Sb}_{22}\text{Te}_{56}$  film. This means that FCC phases of  $\text{Ge}_{22}\text{Sb}_{22}\text{Te}_{56}$  is more stable after Ag is added. This may be because the doped Ag atom substitutes for the Ge, Sb, Te atoms or vacancies in  $\text{Ge}_{22}\text{Sb}_{22}\text{Te}_{56}$  film, or form compounds with the Ge, Sb, or Te atoms. The above three reasons all will form a more stable FCC phases and also increase the phase-transformation temperature of the FCC to HCP phase. Curve c and d in Fig. 2 shows the diffractogram of  $\text{Ge}_{22}\text{Sb}_{22}\text{Te}_{56}$  and Ag-photodoped  $\text{Ge}_{22}\text{Sb}_{22}\text{Te}_{56}$  films annealed at  $250^\circ\text{C}$  respectively. Peaks

of (102), (103) and (110) planes [14] of HCP structure of  $\text{Ge}_2\text{Sb}_2\text{Te}_3$  (GST) are identified and also the planes of  $\text{Sb}_2\text{Te}_3$  are found in the annealed films. Peaks of (310) and (510) planes of  $\text{Ag}_5\text{Te}_3$  phases are identified by using JCPDS database (1997) in Ag-photodoped films.

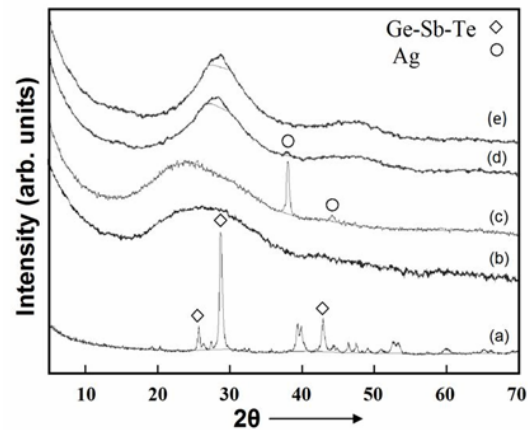


Fig. 1. X-ray diffraction patterns for (a)  $\text{Ge}_{22}\text{Sb}_{22}\text{Te}_{56}$  bulk alloy, (b) as deposited  $\text{Ge}_{22}\text{Sb}_{22}\text{Te}_{56}$  thin film, (c) Ag film on the glass substrate (d) Ag: $\text{Ge}_{22}\text{Sb}_{22}\text{Te}_{56}$  bilayer without light exposure (e) After 20 min. illumination of Ag: $\text{Ge}_{22}\text{Sb}_{22}\text{Te}_{56}$ .

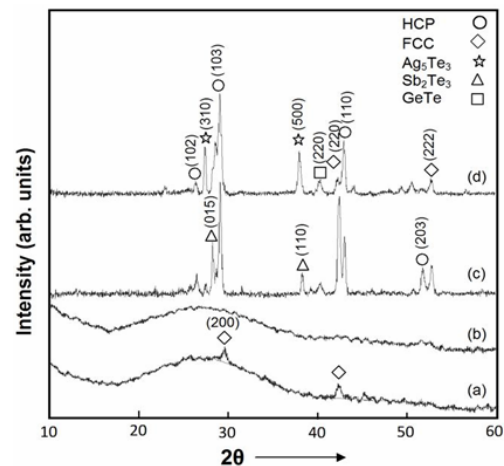


Fig. 2. XRD scan for the films annealed at  $160^\circ\text{C}$  (a), (b) for  $\text{Ge}_{22}\text{Sb}_{22}\text{Te}_{56}$  and  $\text{Ge}_{22}\text{Sb}_{22}\text{Te}_{56}:\text{Ag}$  films respectively and at  $250^\circ\text{C}$  (c), (d) for  $\text{Ge}_{22}\text{Sb}_{22}\text{Te}_{56}$  and  $\text{Ge}_{22}\text{Sb}_{22}\text{Te}_{56}:\text{Ag}$  films respectively.

Fig. 3 shows the sheet resistance values of  $\text{Ge}_{22}\text{Sb}_{22}\text{Te}_{56}$  and Ag-photodoped  $\text{Ge}_{22}\text{Sb}_{22}\text{Te}_{56}$  films, at a heating rate of  $2^\circ\text{C}/\text{min}$ . A continuous decrease in resistivity is observed followed by an abrupt drop at  $160^\circ\text{C}$  and  $175^\circ\text{C}$  for  $\text{Ge}_{22}\text{Sb}_{22}\text{Te}_{56}$  and Ag-photodoped  $\text{Ge}_{22}\text{Sb}_{22}\text{Te}_{56}$  films respectively. The presence of the abrupt drop in resistance with temperature is characteristic of Ge-Sb-Te system and indicates that the Ge-Sb-Te system is present as a continuous network in the whole of

the sample and is mainly responsible for electrical conduction. The model presented by Kolobov provides a clear explanation of rapid amorphous-crystalline transformation in Ge-Sb-Te system [15]. In  $\text{Ge}_2\text{Sb}_2\text{Te}_5$ , Te atoms form FCC lattice and Ge occupies octahedral and tetrahedral positions in the crystalline and amorphous states respectively. At amorphous to crystalline transformation temperature, with the rupture of weak bonds Ge flips into the tetrahedral position. Whereas on melting the Ge atom undergoes a reverse (umbrella) flip to octahedral position resulting in the distortion of the Ge sublattice [16]. This rapid amorphous-crystalline transformation appears as an abrupt drop in resistance in temperature dependent sheet resistance measurements. For Ag-photodoped  $\text{Ge}_{22}\text{Sb}_{22}\text{Te}_{56}$  film phase transformation temperature increases, this is further confirmed by x-ray diffraction studies reported in previous section. The reduction in resistance upon phase change is more than three orders of magnitude in both cases. The local arrangement of atoms around Sb remains essentially unchanged. The Sb atoms mainly play the role of enhancing overall stability of the metastable crystal structure by participating in the overall electron balance [16].

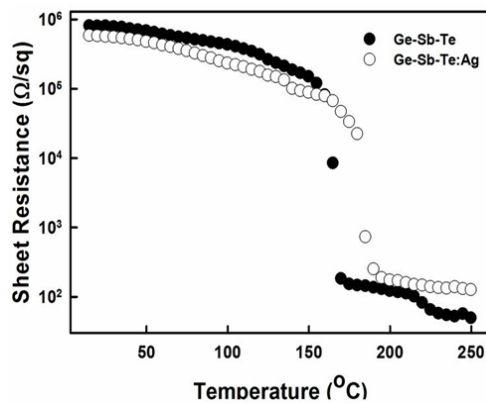


Fig. 3. Sheet resistance variation with temperature for as deposited  $\text{Ge}_{22}\text{Sb}_{22}\text{Te}_{56}$  and Ag-Photodoped  $\text{Ge}_{22}\text{Sb}_{22}\text{Te}_{56}$  films.

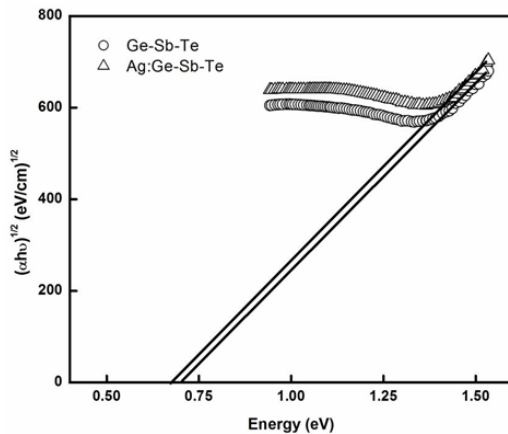


Fig. 4. Plots of  $(ahv)^{1/2}$  vs.  $hv$  for  $\text{Ge}_{22}\text{Sb}_{22}\text{Te}_{56}$  and Ag-photodoped  $\text{Ge}_{22}\text{Sb}_{22}\text{Te}_{56}$  films.

The absorption coefficient ( $\alpha$ ) of the films has been calculated from the transmission ( $T$ ) and reflection ( $R$ ) data using the relation [17]:

$$\alpha = \left(\frac{1}{t}\right) \ln \left\{ \frac{(1-R^2)}{(2T)} + \left[ \frac{(1-R^2)}{(2T)^2} + R^2 \right]^{1/2} \right\} \quad (1)$$

Where  $t$  is the thickness of the films,  $T$  and  $R$  represent the transmission and reflection percentage respectively.

According to Tauc [18] it is possible to separate three distinct regions in the absorption edge spectrum of amorphous semiconductors. The first is the weak absorption tail, which originates from the defect and impurities, the second is the exponential edge region, which is strongly related to the randomness of the system and the third is the high absorption region, involving that's determines the optical energy gap. In the high absorption region, involving indirect interband transitions between valence and conduction bands,  $\alpha$  follows the relation:

$$\alpha hv = B(hv - E_{op})^2 \quad (2)$$

where  $E_{op}$  is the optical band gap and  $B$  is a constant, which is a measure of the extent of band tailing. A plot of  $(\alpha hv)^{1/2}$  versus  $hv$  gives a straight line, whose intercept on the energy axis gives  $E_{op}$  and whose slope gives the value of constant  $B^{1/2}$ . Plots of  $(\alpha hv)^{1/2}$  versus  $hv$  for  $\text{Ge}_{22}\text{Sb}_{22}\text{Te}_{56}$  and Ag-photodoped  $\text{Ge}_{22}\text{Sb}_{22}\text{Te}_{56}$  compositions are shown in Fig. 3. The calculated values of the optical band gap  $E_{op}$  and the approximate values of the band tailing parameter  $B^{1/2}$  are shown in Table 1. It is observed in Fig. 3 and Table 1, the  $E_{op}$  of the as deposited  $\text{Ge}_{22}\text{Sb}_{22}\text{Te}_{56}$  and Ag-photodoped  $\text{Ge}_{22}\text{Sb}_{22}\text{Te}_{56}$  films is approximately 0.70 and 0.67 eV, respectively. In case of amorphous  $\text{Ge}_{22}\text{Sb}_{22}\text{Te}_{56}$  film, this  $E_{op}$  value is in good agreement with those reported in some other papers [19, 20]. The slope quantities  $B^{1/2}$  as-deposited  $\text{Ge}_{22}\text{Sb}_{22}\text{Te}_{56}$  film is  $811.60 \text{ cm}^{-1/2} \text{ eV}^{-1/2}$  exhibit a small decrease in comparison to those of Ag-photodoped  $\text{Ge}_{22}\text{Sb}_{22}\text{Te}_{56}$  films. That is, the additive Ag decreases the  $E_{op}$  of the amorphous  $\text{Ge}_{22}\text{Sb}_{22}\text{Te}_{56}$  film ( $\Delta E_{op} \sim 0.03 \text{ eV}$ ) while causing an increase in  $B^{1/2}$ . In particular, an increase in slope is due to the decrease in randomness in the atomic configuration [19].

Table 1. The quantities  $T_c$ ,  $E_{op}$  and  $B^{1/2}$  of as-deposited  $Ge_{22}Sb_{22}Te_{56}$  and Ag-photodoped  $Ge_{22}Sb_{22}Te_{56}$  films.

Composition		$E_{op}$ (eV)	$B^{1/2}$ ( $cm^{-1/2} eV^{-1/2}$ )	$T_c$ ( $^{\circ}C$ )
$Ge_{22}Sb_{22}Te_{56}$	As-deposited	0.70	811.60	160
$Ge_{22}Sb_{22}Te_{56}:Ag$	As-deposited	0.67	815.18	175

#### 4. Conclusions

The structural, optical and electrical properties of  $Ge_{22}Sb_{22}Te_{56}$  and Ag-photodoped  $Ge_{22}Sb_{22}Te_{56}$  films were analyzed. The as-prepared, Ag-photodoped films are amorphous and crystallize into a mixture of  $Ge_2Sb_2Te_5$ ,  $Sb_2Te_3$  and GeTe phases upon annealing. The XRD and sheet resistance data reveal that the phase change of  $Ge_{22}Sb_{22}Te_{56}$  and Ag-photodoped  $Ge_{22}Sb_{22}Te_{56}$  films is a two-step process (amorphous  $\rightarrow$  fcc  $\rightarrow$  hexagonal) but Ag-photodoped  $Ge_{22}Sb_{22}Te_{56}$  films shows the increase in transformation temperature of 160  $^{\circ}C$  for the amorphous-to-crystalline transformation of  $Ge_{22}Sb_{22}Te_{56}$  films. The phases of  $Ag_5Te_3$  are formed in Ag-photodoped film during crystallization. It is found that optical gap decreases and band tailing parameter increases with addition of Ag in the alloy. The marginal increase in the band tailing suggests the decrease in the randomness of the alloy. Thus photodiffusion of Ag into the ternary chalcogenide matrix introduced new Ag-Te bonds, which exhibits the change in phase transformation temperature, optical gap and band tailing parameter.

#### Acknowledgements

The authors are grateful to CSIR for the sanctioning of SRF (NET) to one of the authors and for funding a project (03/1140/09/EMR-11). The authors also wish to thank Dr. T. Shripathi (Scientist G) and Mr. U. Deshpande UGC-DAE Consortium for Scientific Research Indore, India for providing access to the UV-VIS-NIR facility.

#### References

- [1] N. Yamada, E. Ohno, K. Nishiuchi, N. Akahira, J. Appl. Phys. **69**, 2849 (1991).
- [2] J. Y. Park, J. Y. Lee, M. S. Youm, Y. T. Kim, H. S. Lee, J. App. Phys. **97**, 093506 (2005).
- [3] C. T. Lie, P. C. Kuo, W. C. Hsu, T. H. Wu, P. W. Chen, S. C. Chen, Jpn. J. Appl. Phys. **42**, 1026 (2003).

- [4] K. Wang, D. Wamwangi, S. Ziegler, C. Steimer, and M. Wuttig, J. App. Phys. **96**, 5557 (2004).
- [5] K. Wang, C. Steimer, D. Wamwangi, S. Ziegler, M. Wuttig, Appl. Phys. A **80**, 1611 (2005).
- [6] M. Frumar, T. Wagner, Curr. Opin. Solid State Mater. Sci. **7**, 117 (2003).
- [7] M. Kalyva, A. Siokou, S. N. Yannopoulos, T. Wagner, Krbal, J. Orava, M. Frumar, J. App. Phys. **104**, 043704 (2008).
- [8] D. Singh, S. Kumar, R. Thangaraj, J. Optoelectron. Adv. Mater., **12**, 1706 (2010).
- [9] D. Singh, S. Kumar, R. Thangaraj, J. Optoelectron. Adv. Mater., **12**(7), 1505 (2010).
- [10] D. Singh, S. Kumar, R. Thangaraj, J. Optoelectron. Adv. Mater., **12**(11), 2242 (2010).
- [11] M. Abkowitz, Polym. Eng. Sci. **24**, 1149 (1984).
- [12] M. Mitkova, M. N. Kozicki, H.C. Kim, T. L. Alford, Thin solid films **449**, 248 (2004).
- [13] C. A. Lucas, J. Phys. D: Appl. Phys. **24**, 928 (1991).
- [14] W. K. Njoroge, Ph.D thesis, Rheinisch-Westfalischen Technical University, Aachen (2001).
- [15] A. V. Kolobov, P. Fons, A. I. Frenkel, A. L. Ankudinov, J. Tominaga, T. Uruga, Nature Mater. **3**, 703 (2004).
- [16] A. V. Kolobov, P. Fons, J. Tominaga, A. I. Frenkel, A. L. Ankudinov, S. N. Yannopoulos, K. S. Andrikopoulos, T. Uruga, Jpn J. Appl. Phys. **44**, 3345 (2005).
- [17] G. Lucovsky, Phys. Rev. B **15**, 5762 (1977).
- [18] J. Tauc, Amorphous and Liquid Semiconductors (Plenum Press, London, 1974).
- [19] K. H. Song, S. W. Kim, J. H. Seo, H. Y. Lee, J. App. Phys. **104**, 103516 (2008).
- [20] B. S. Lee, J. R. Abelson, S. G. Bishop, D. H. Kang, B. K. Cheong, J. Appl. Phys. **97**, 093509 (2005).

\*Corresponding author: rthangaraj@rediffmail.com